We are IntechOpen,
the world's leading publisher of
Open Access books
Built by scientists, for scientists

6,900
Open access books available

185,000
International authors and editors

200M
Downloads

154
Countries delivered to

Our authors are among the

TOP 1%
most cited scientists

12.2%
Contributors from top 500 universities

BOOK CITATION INDEX
CLARIVATE ANALYTICS
INDEXED

WEB OF SCIENCE™

Selection of our books indexed in the Book Citation Index
in Web of Science™ Core Collection (BKCI)

Interested in publishing with us?
Contact book.department@intechopen.com

Numbers displayed above are based on latest data collected.
For more information visit www.intechopen.com

Filter Band Multicarrier Based Transmission Technology for Clinical EEG Signals

Chin-Feng Lin, Wei-Syuan Chao and Jun-Da Chen

Additional information is available at the end of the chapter

Abstract

A transmission scheme is proposed based on filter band multicarrier (FBMC) transmission technology for clinical electroencephalogram (EEG) signals. The proposed scheme integrates binary phase shift keying (BPSK) and offset quadrature amplitude modulation (OQAM), an FBMC transmission mechanism, and low-density parity-check code (LDPC) error protection in an FBMC-based EEG mobile communication system. The proposed EEG mobile communication system employs high-speed transmission, with schemes providing significant error protection for mobile communication of clinical EEG signals requiring a stringent bit-error rate (BER). The performances of BERs and mean square errors (MSEs) of the proposed EEG mobile communication system were explored. Simulation results show that the proposed scheme is a superior transmission platform as compared to existing schemes for clinical EEG signals.

Keywords: EEG, FBMC, OQAM, LDPC

1. Introduction

Noninvasive monitoring of brain activity in daily life is an important research topic in the field of healthcare that aims at a comfortable lifestyle. Mihajlovic et al. [1] demonstrated various aspects of wireless and intelligent wearable lifestyle electroencephalogram (EEG) solutions, and the technology behind the development of convenient, intelligent, and wearable, wireless EEG devices was explored. In addition, in their study, personality traits, sensory input, neuronal activity, conductive tissues, electrode-tissue interface, miniaturized and ergonomic EEG headsets, wireless and wearable EEG system designs, brain activity analysis, and output interfaces were discussed. Lin et al [2] proposed a Bluetooth-based real-time brain-computer

interface (BCI) system that can be used to detect drowsiness while driving. This system had integrated wireless physiological signal-acquisition and embedded signal-processing modules, and it featured real-time wireless drowsiness detection, long-term daily life EEG monitoring, high computation capacity, and low power consumption. The design and implementation of a Bluetooth-based wearable brain monitoring system was investigated by Sawan et al. [3]. A wireless data recording system was utilized for noninvasive and long-term monitoring of near-infrared spectrometry (NIRS) EEG signals. In addition, the wireless data recording system was applied to the field of invasive cerebral EEG detection. This system has a graphical user interface that is user-friendly and can be used to extract brain activity during dynamic tasks. The advantages of the designed system are portability, wireless connectivity, high throughput, reliable communication, and low-power consumption. Liao et al. [4] proposed a design method for the 16-channel EEG measurement system utilizing dry spring-loaded sensors, a Bluetooth-based acquisition system, and a size-adjustable wearable soft cap. Vos et al. [5] demonstrated an efficient low-cost mobile EEG system that utilizes a P300-based speller for wireless BCI.

The development of high-speed, and reliable EEG transmission schemes are interesting research topics. Channel coding is a solution that can be used to achieve a lower error probability for EEG communication. The fundamental design parameters of channel coding are error probability, complexity, and decoding time. Low-density parity-check (LDPC) code is a channel coding technology that was proposed by Gallager [6]. Limpaphayom et al. [7] proposed a power and bandwidth-efficient communication system that utilizes irregular LDPC component codes of block length 100,000, multilevel coding, multistage decoding, 64-quadrature amplitude modulation, and trellis-based signal shaping schemes. The proposed system achieved a bit-error rate (BER) of 10^{-5} at an Eb/No of 6.55 dB. Franceschini et al. [8] described the concept of LDPC codes. The regular (v, c) LDPC codes are linear block codes with a sparse parity-check matrix H, In H, the number of nonzero elements in the columns is v, while the number of nonzero elements in the rows is c. In addition, the code rate is defined as $1 - v/c$. In an (N,K) LDPC code, the block length is N and the information length is K. Ohtsuki [9] applied LDPC codes to various transmission systems with excellent performance, and illustrated some of the LDPC code designs. LDPC codes are included in the second-generation specification for satellite broadband applications, and in IEEE 802.16e.

Filter bank-based multicarrier modulations (FBMC) is an interesting research topic, and it is being considered as a potential candidate for the fifth generation (5G) mobile systems. FMBC is a modified version of orthogonal frequency division multiplexing (OFDM), and a tutorial review of FBMC modulations was discussed by Boroujeny et al. [10]. Compared to cyclic prefix (CP)-based OFDM modulation, FBMC offers better spectral efficiency in multipath channels. Bouhadda et al. investigated the BER performance of nonlinear distortion in high-power amplifiers for FBMC using offset quadrature amplitude modulation (OQAM) [11]. Caus et al. [12] studied the effects of multi-tap filtering on FBMC/OQAM systems to combat inter-symbol and inter-carrier interferences due to multipath fading. Caus et al. [12] proposed a low-complexity transmission power estimation method, and their simulation results show that the proposed transmission power estimation method is excellent. Further, Bellanger et al. [13] proposed an FBMC-based physical layer solution for 5G mobile systems.

In previous studies, a survey study of mobile telemedicine [14], mobile telemedicine using an advanced wireless multimedia communication application [15], an 802.11n wireless telemedicine application [16], a direct sequence ultra-wideband (DS-UWB) wireless telemedicine application [17], a multi-code code division multiple access (CDMA) mobile medicine system [18], a Ka band OFDM-based multi-satellite mobile telemedicine system [19], a Ka band wideband CDMA mobile telemedicine system [20], and a mobile cloud-based blood pressure healthcare system [21] were investigated. In this chapter, an advanced FBMC-based EEG transmission scheme is proposed. The design concept of the proposed advanced wireless EEG transmission system includes FBMC, LDPC, BPSK or OQAM, and a power assignment mechanism. Low power high-speed wireless EEG transmission was achieved.

2. System model

The proposed FBMC-based EEG transmission scheme is shown in **Figure 1**. The LDPC channel coding, FBMC transmission method, a BPSK or OQAM adaptive modulation, and a power assignment mechanism were used in a new design strategy to achieve low power, high speed, and high quality of service transmission capabilities for wireless EEG systems. We performed a simulation using the irregular LDPC codes set with a block length of 2000 and a rate of 1/2. The digital bit streams of the EEG signal were inputted to the irregular LDPC encoder, and the LDPC bit streams were outputted. The OQAM modulation scheme is used at the lower fading channel in order to achieve high-speed wireless EEG transmission. A BPSK is used at the highest fading channel, to achieve robust EEG communication. The LDPC bit streams were inputted to an OQAM-based or BPSK-based adaptive modulator, and the LDPC bit streams with adaptive modulation were outputted. The LDPC bit streams with adaptive modulation were inputted to the serial to parallel converter, and the 64 parallel LDPC adaptive modulation EEG bit streams were outputted. The 64 parallel LDPC adaptive modulation EEG bit streams were inputted to the digital filter banks (DFBs). The coefficients of the DFBs were determined to be as follows [13].
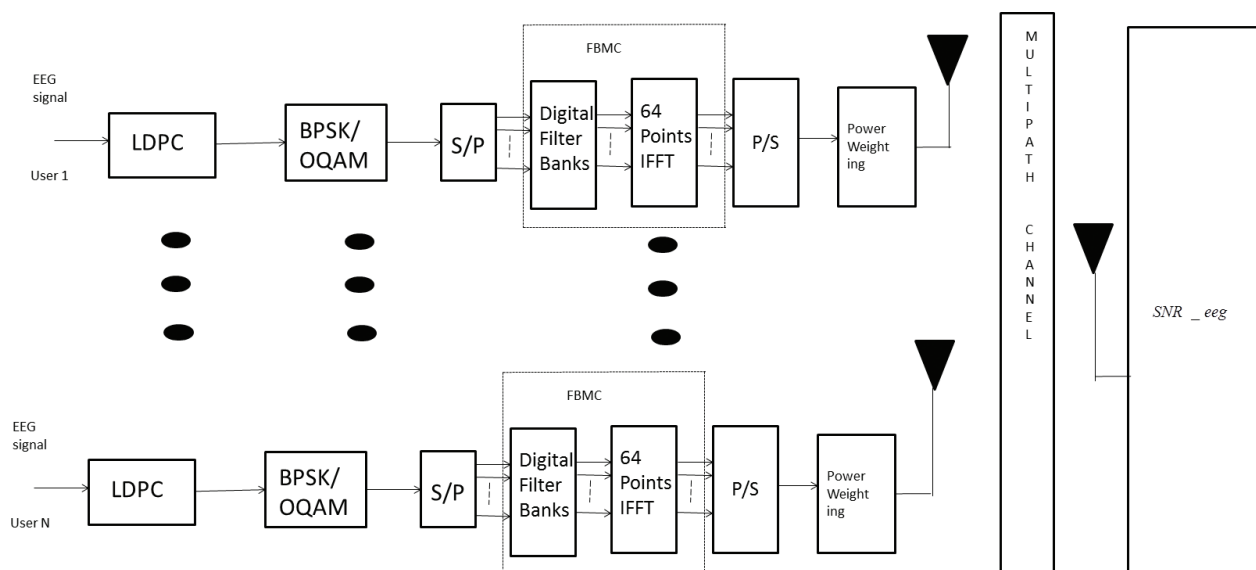

Figure 1. The proposed FBMC-based EEG transmission scheme.

$$H_0 = 1, H_1 = 0.971960, H_2 = \sqrt{2}/2, H_3 = 0.235147 \tag{1}$$

Further, the 64 DFB output bit streams were inputted to a 64-point inverse fast Fourier transform (IFFT), and the 64 parallel LDPC adaptive modulation FBMC EEG bit streams were outputted. The 64 parallel LDPC adaptive modulation FBMC EEG bit streams were inputted to a parallel to serial converter, and the serial LDPC adaptive modulation FBMC EEG bit streams were output. The proposed power assignment algorithm is summarized below:

Step 1: On the basis of the output information obtained from the object-component Petri Nets (OCPN) model, determine throughputs for EEG packets transmission.

Step 2: Select the appropriate modulation mode to satisfy the requirements for transmission over a wireless EEG transmission system.

Step 3: Assign the initial value of power weighting as 15/30 for EEG packets.

Step 4: Measure the received signal to noise ratio (SNR) for EEG packets.

Step 5: If the measured SNR of the received signal exceeds the threshold SNR at which the required BER for EEG packets is achieved, then update the power weighting as power weighting = power weighting − 1/30; If power weighting ≥1/30, go to Step 4; otherwise, go to Step 7.

Step 6: If the measured SNR of the received signal is less than the threshold SNR at which the required BER for EEG packets is achieved, then update the power weighting as power weighting = power weighting + 1/30; If power weighting ≤1, go to Step 4; otherwise, go to Step 8.

Step 7: Change the modulation mode. If the modulation mode is not OQAM, go to Step 4.

Step 8: Increase the modulation mode. If the modulation mode is not BPSK, go to Step 4.

The carrier sense multiple access with collision avoidance (CSMA/CA) technology were used for multiuser wireless EEG transmission system.

3. Simulation Results

Figure 2 shows the original EEG signal, and the clinical test signal is an original alcoholic EEG (lead FP1) (http://kdd.ics.uci.edu/databases/eeg). The length of the clinical EEG signal is 50 s, and the sampling rate is 256 samples/s. **Figure 3** shows the received EEG signal with a BER of 10^{-7} and a mean square error (MSE) of 9.76×10^{-10}. The MSE was defined as following:

$$MSE = \frac{\sum_{i=1}^{N}(x_i - y_i)^2}{N} \tag{2}$$

x_i: the original EEG signal.

y_i: the received EEG signal.
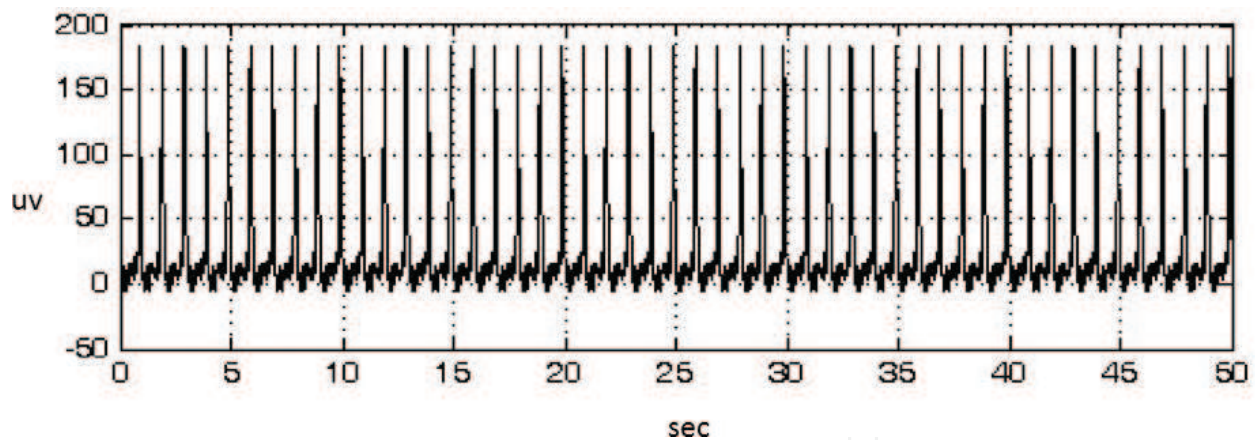
N: the length of original EEG signal.

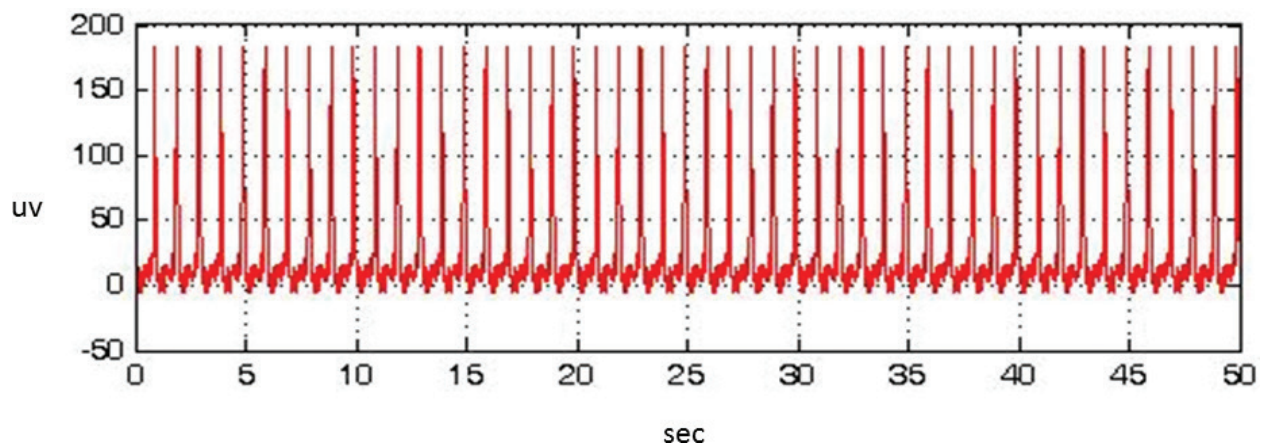**Figure 2.** The original EEG signal.

Figure 3. The received EEG signal with a BER of 10^{-7} and an MSE of 9.76×10^{-10}.

The block length of 2000 and rate of 1/2 irregular LDPC encoder, BPSK, and 64-points IFFT were used in the simulation, and the coefficients of the tap-delay line multipath channel model were [1, 0.5, 0.25, 0.125]. The assumed coefficients of multipath channel estimation (ACMCE) were [0.99, 0.495, 0.2475, 0.12375]. **Figure 4** shows the received EEG signal with a BER of 2.5×10^{-6} and an MSE of 5.24×10^{-5}. **Figure 5** shows the received EEG signal with a BER of 2.5×10^{-5} and an MSE of 1.32×10^{-2}. There was no difference on the human vision. **Figure 6** shows the received EEG signal with a BER of 1.7×10^{-3} and an MSE of 0.21. **Figure 7** shows the received EEG signal with a BER of 8.8×10^{-3} and an MSE of 1044.10. There were obviously differences on the human vision.

Our BER performance results for the proposed wireless EEG transmission system are shown in **Figure 8**. The six signs "△," "□," "o," "☆," "*," and "x" denote the ACMCE with no error using BPSK, ACMCE with no error using OQAM, ACMCE with 1% error using BPSK, ACMCE with 1% error using OQAM, ACMCE with 10% error using BPSK, and ACMCE with 10% error using OQAM, respectively. As shown in the figure, the BER of BPSK was smaller than that of OQAM. Furthermore, the BER of the ACMCE with 10% error was larger than that of the ACMCE with no error. The MSE performance results for the proposed wireless EEG
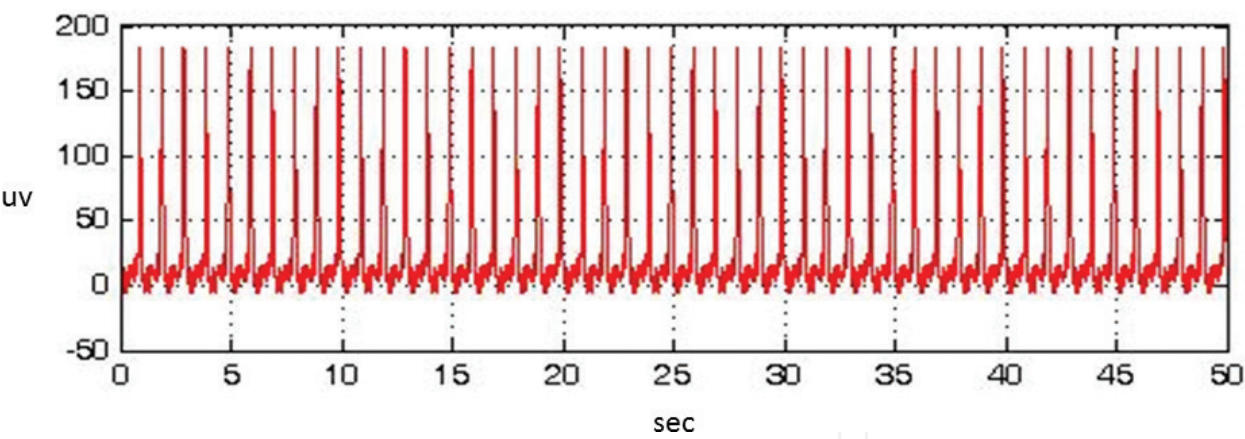
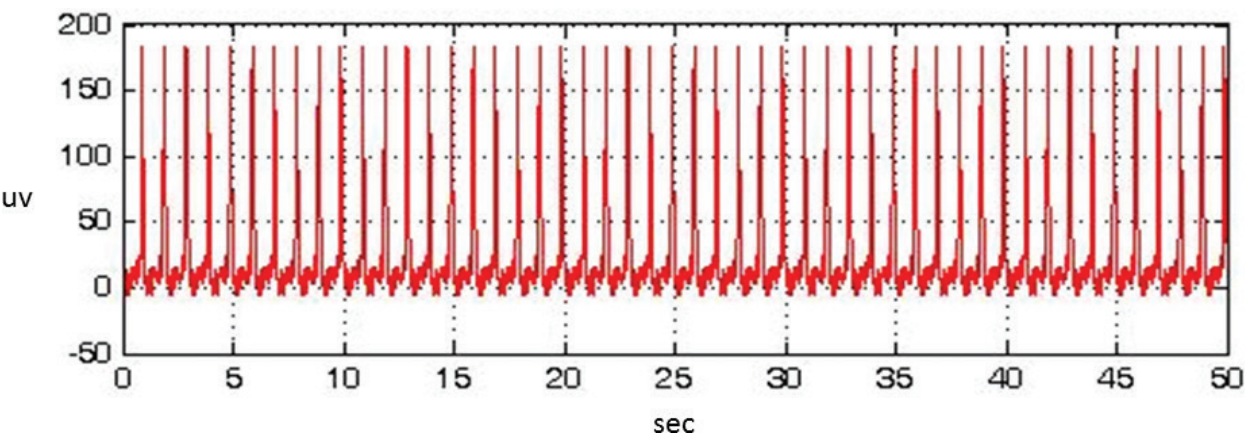**Figure 4.** The received EEG signal with a BER of 2.5×10^{-6} and an MSE of 5.24×10^{-5}.

Figure 5. The received EEG signal with a BER of 2.5×10^{-5} and an MSE of 1.32×10^{-2}.

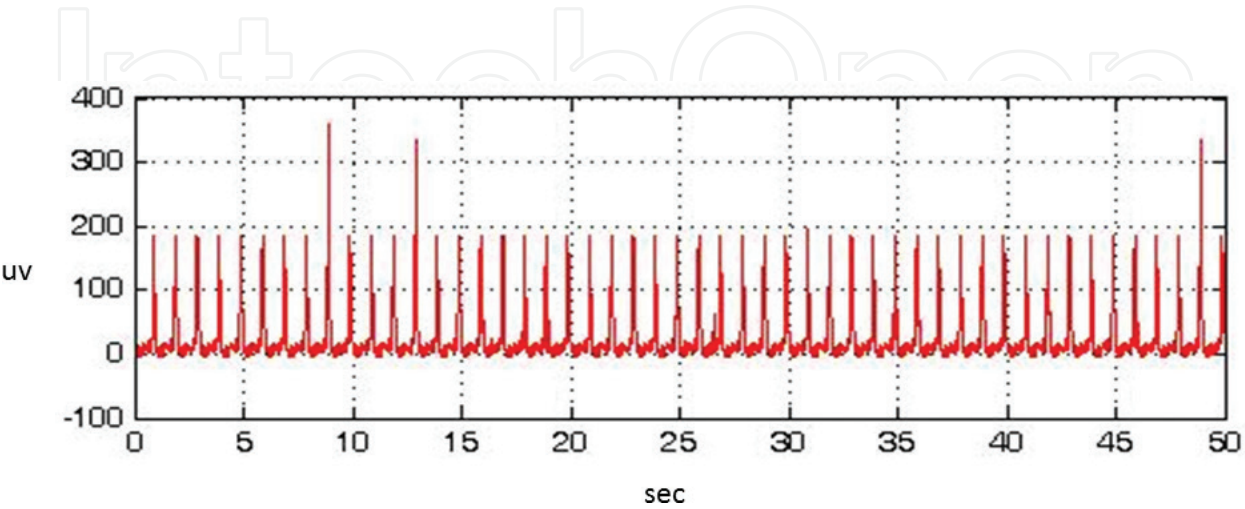**Figure 6.** The received EEG signal with a BER of 1.7×10^{-3} and an MSE of 0.21.
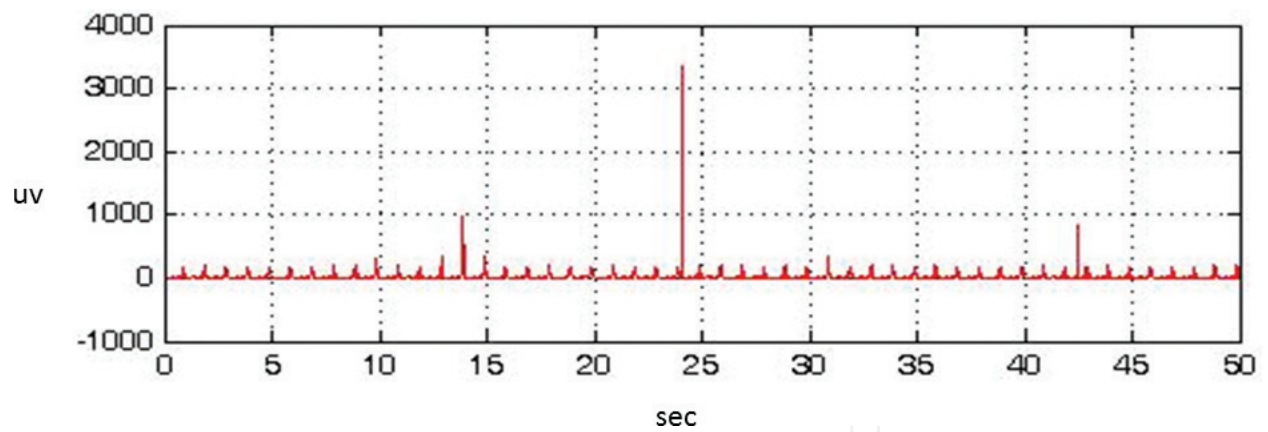
Figure 7. The received EEG signal with a BER of 8.8×10^{-3} and an MSE of 1044.10.
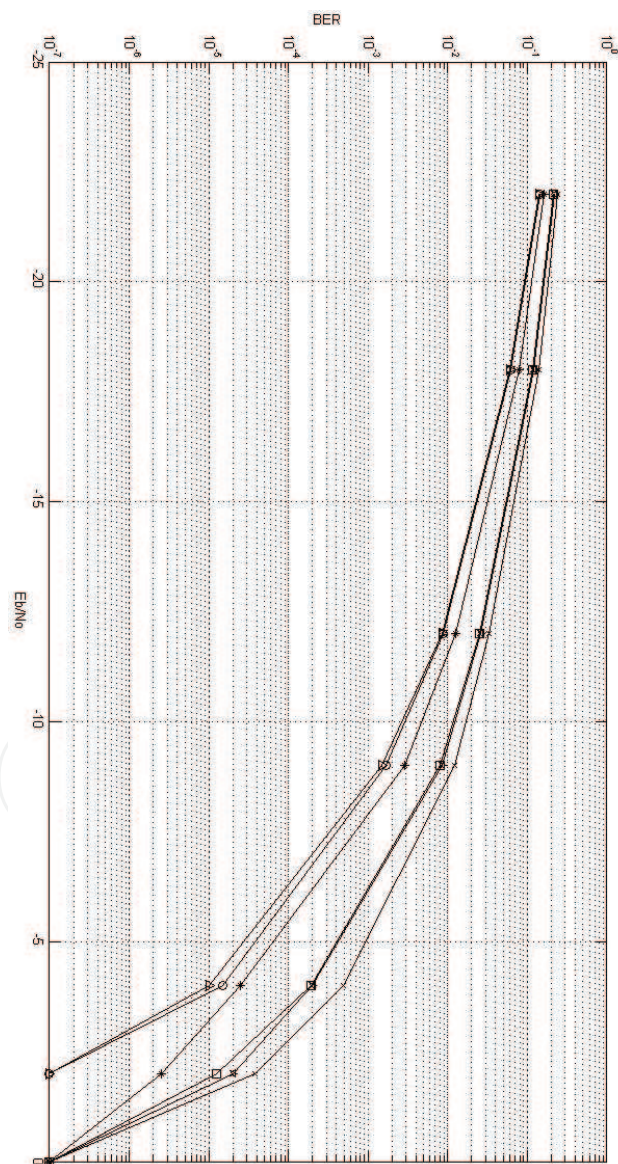

Figure 8. The BER performance results for the proposed wireless EEG transmission system.

transmission system are shown in **Figure 9**. The six signs "△," "□," "o," "☆," "*," and "x" denote the ACMCE with no error using BPSK, ACMCE with no error using OQAM, ACMCE with 1% error using BPSK, ACMCE with 1% error using OQAM, ACMCE with 10% error using BPSK, and ACMCE with 10% error using OQAM, respectively. As shown in the figure, the MSE of BPSK was smaller than that of OQAM. Furthermore, the MSE of the ACMCE with 10% error was larger than that of the ACMCE with no error. The relations of transmission power and noise power are shown in **Figure 10**. The signal to noise ratio, Eb/No, was defined as following:

$$\frac{E_b}{N_o} = \frac{transmission \quad power}{noise \quad power} \tag{3}$$

$$E_b : transmission \quad power$$
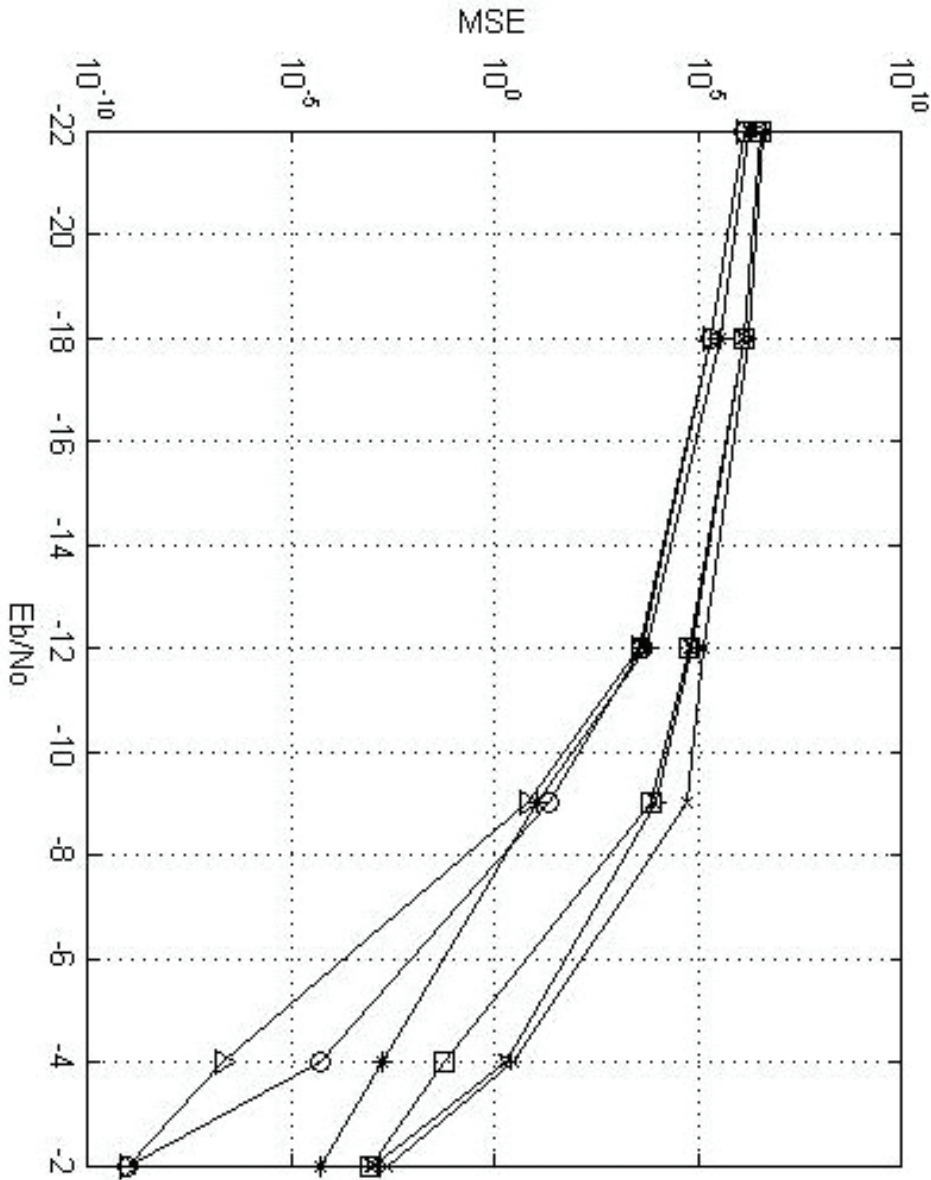
$$N_o : noise \quad power$$

Figure 9. The MSE performance results for the proposed wireless EEG transmission system.

The transmission BER was 10^{-7}. The four signs "o," "x," "$\triangle$," and "$\star$," denote the ACMCE with no error using BPSK, ACMCE with no error using OQAM, ACMCE with 15% error using BPSK, and ACMCE with 15% error using OQAM, respectively. When noise power was fixed, the transmission power of ACMCE with 15% error using OQAM was the highest, the transmission power of ACMCE with 15% error using BPSK was the second highest, the transmission power of ACMCE with no error using OQAM was the third highest, and the transmission power of ACMCE with no error using BPSK was the lowest. The relation of ratios of the saving transmission power and noise power were shown in **Figure 11**. The saving in transmission power was defined as following:

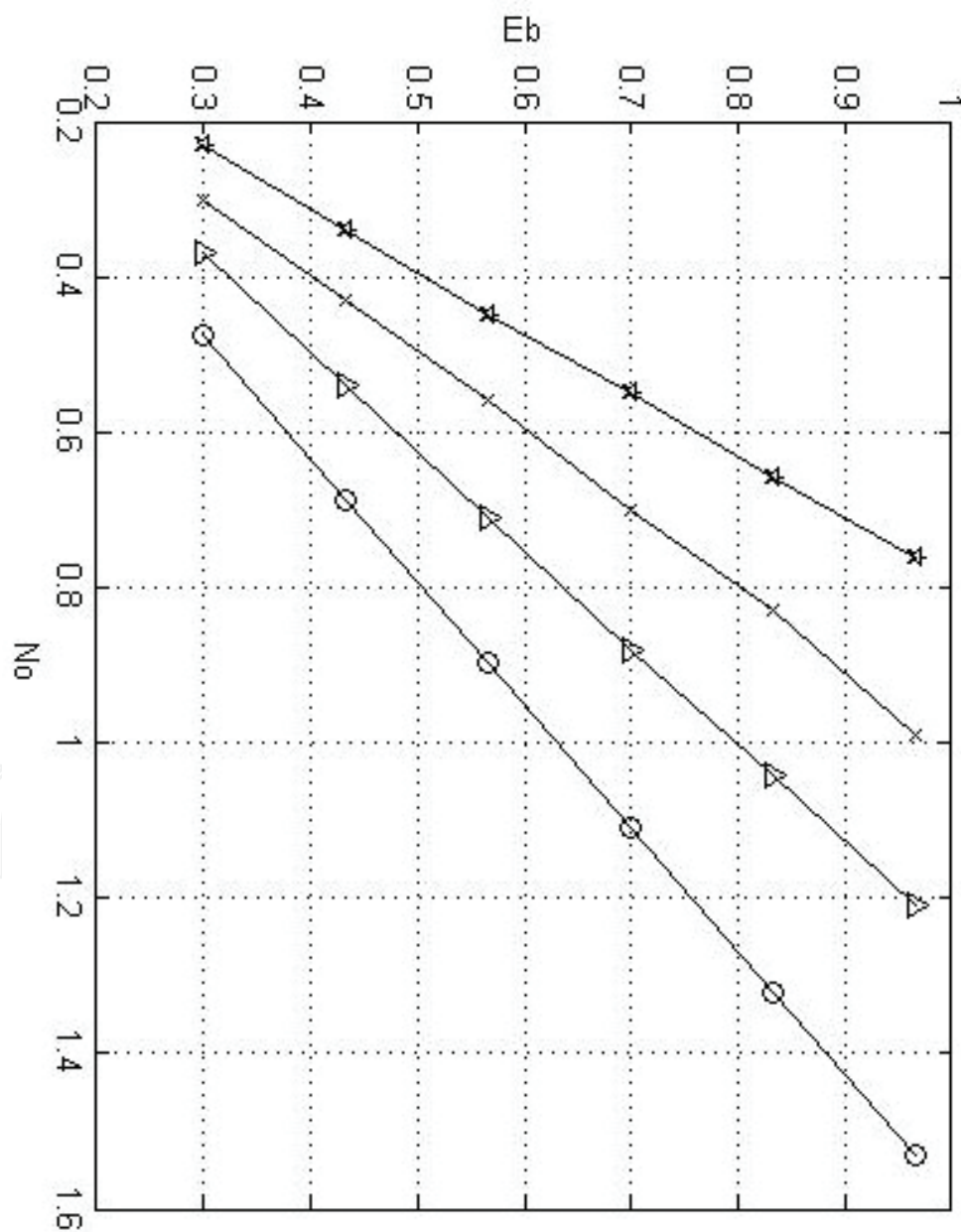$$power \quad saving \ = \ (1 - E_b) * 100\% \tag{4}$$

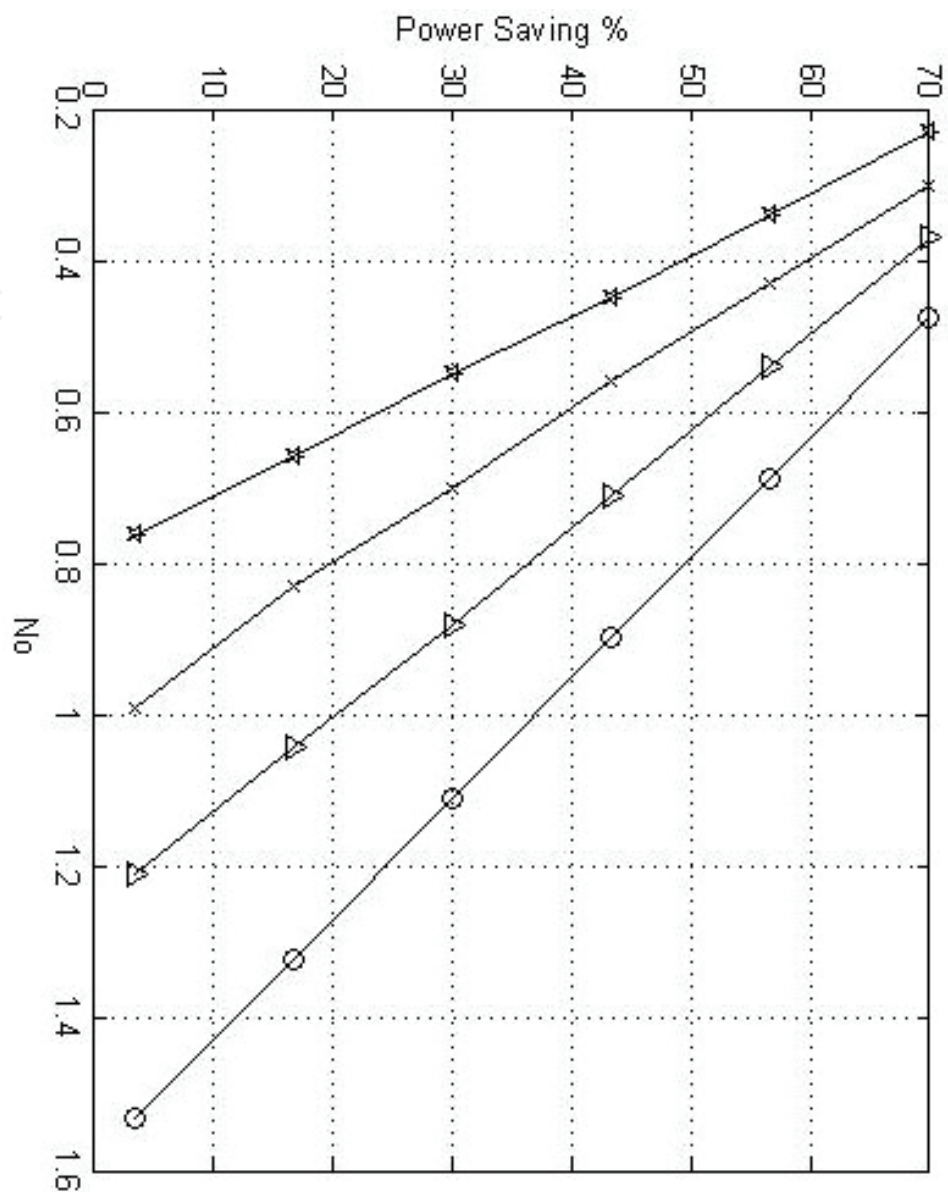**Figure 10.** The relations of transmission power and noise power.

Figure 11. The relation of ratios of the saving transmission power and noise power.

The transmission BER was 10^{-7}. The four signs "o," "x," "△," and "☆," denote the ACMCE with no error using BPSK, ACMCE with no error and OQAM, ACMCE with 15% error and BPSK, using ACMCE with 15% error and OQAM, respectively. When noise power was fixed, the transmission power saving of ACMCE with 15% error using OQAM was the lowest, the transmission power saving of ACMCE with 15% error using BPSK was the second lowest, the transmission power saving of ACMCE with no error using OQAM was the third lowest, and the transmission power saving of ACMCE with no error using BPSK was the highest.

4. Conclusion

In this chapter, a new FBMC-based wireless EEG transmission technology was inves-tigated. Advanced LDPC, OQAM and BPSK adaptive modulation, FBMC, wireless

communication methods and a power assignment mechanism were integrated. Simulation results were obtained for a variety of received EEG signals, with a range of BER results. The BER performances of the proposed wireless EEG transmission architectures and the MSE performances of the proposed wireless EEG transmission architectures were demonstrated. The beneficial effects of the ACMCE errors were indicated. When the transmission BERs were 10^{-7}, the relationship between transmission power and noise power, and the relationship between the saving transmission power ratios and noise power were discussed. The simulation results confirm that the proposed transmission system is an excellent wireless EEG platform that provides the high speed and low power consumption benefits sought.

Acknowledgements

Author details

Chin-Feng Lin*, Wei-Syuan Chao and Jun-Da Chen

*Address all correspondence to: lcf1024@mail.ntou.edu.tw

Department of Electrical Engineering, National Taiwan Ocean University, Taiwan

References

[1] Mihajlovic V, Grundlehner B, Vullers R, et al. Wearable, wireless EEG solutions in daily life applications: What are we missing? IEEE Journal of Biomedical and Health Informatics. 2015;**19**(1):6-21. DOI: 10.1109/JBHI.2014.2328317

[2] Lin CT, Chang CJ, Lin BS, et al. A real-time wireless brain–computer interface system for drowsiness detection. IEEE Transactions on Biomedical Circuits and Systems. 2010;**4**(4):214-222. DOI: 10.1109/TBCAS.2010.2046415

[3] Sawan M, Salam MT, Lan IL, et al. Wireless recording systems: From noninvasive EEG-NIRS to invasive EEG devices. IEEE Transactions on Biomedical Circuits and Systems. 2013;**7**(2):186-195. DOI: 10.1109/TBCAS.2013.2255595

[4] Liao LD, Wu SL, Liou CH, et al. A novel 16-channel wireless system for electroencephalography measurements with dry spring-loaded sensors. IEEE Transactions on Instrumentation and Measurement. 2014;**63**(6):1545-1555. DOI: 10.1109/TIM.2013.2293 222

[5] De Vos M, Kroesen M, Emkes R, et al. P300 speller BCI with a mobile EEG system: Comparison to a traditional amplifier Journal of Neural Engineering 2014;**11**:036008. DOI: 10.1088/1741-2560/11/3/036008

[6] Gallager RG. Low-Density Parity-Check Codes. Cambridge, MA: MIT Press; 1963

[7] Limpaphayom P, Winick KA. Power- and bandwidth-efficient communications using LDPC codes. IEEE Transactions on Communications. 2004;**52**(3):350-354. DOI: 10.1109/TCOMM.2004.823565

[8] Franceschini M, Ferrari G, Raheli R. LDPC Coded Modulations. Springer; Heidelberg, 2009. pp.37-59. DOI: 10.1007/978-3-540-69457-1_3

[9] Ohtsuki T. LDPC codes in communications and broadcasting. IEICE Transactions on Communications. 2007;**E90-B**(3):440-453. DOI: 10.1093/ietcom/e90-b.3.440

[10] Boroujeny BF. OFDM versus filter bank multicarrier. IEEE Transactions on Signal Processing. 2011;**28**(3):92-112. DOI: 10.1109/MSP.2011.940267

[11] Bouhadda H, Shaiek H, Roviras D, et al. Theoretical analysis of BER performance of non-linearly amplified FBMC/OQAM and OFDM signals. EURASIP Journal on Advances in Signal Processing. 2014;**2014**:60. DOI: 10.1186/1687-6180-2014-60

[12] Caus M, Ana I PN, Kliks A. Characterization of the effects of multi-tap filtering on FBMC/OQAM systems. EURASIP Journal on Advances in Signal Processing. 2014;**2014**:84. DOI: DOI: 10.1186/1687-6180-2014-84

[13] Bellanger M, Ruyet DL, Roviras D, et al. Fbmc physical layer: A primer. PHYDYAS. 2010

[14] Lin CF. Mobile telemedicine: A survey study. Journal of Medical Systems. 2012;**36**(2):511-520. DOI: 10.1007/s10916-010-9496-x

[15] Lin CF. An advance wireless multimedia communication application: Mobile telemedicine. WSEAS Transactions on Communications. 2012;**9**(3):206-215

[16] Lin CF, Hung SI, Chiang IH. An 802.11n WLAN transmission scheme for wireless telemedicine applications. Proceedings of the Institution of Mechanical Engineers. Part H, Journal of Engineering in Medicine. 2010;**224**(10):1201-1208. DOI: 10.1177/0954411911434246

[17] Lin CF, Li CY. A DS UWB transmission system for wireless telemedicine. WSEAS Transactions on Systems. 2008;**7**(7):578-588

[18] Lin CF, Chang WT, Lee HW, et al. Downlink power control in multi-code CDMA mobile medicine system. Medical & Biological Engineering & Computing 2006;**44**:437-444. DOI: 10.1007/s11517-009-0458-8

[19] Lin CF, Chang KT. A power assignment mechanism in Ka band OFDM-based multi-satellites mobile telemedicine. Journal of Medical and Biological Engineering. 2008;**28**(1):17-22

[20] Lin CF, Chen JY, Shiu RH, et al. A Ka band WCDMA-based LEO transport architecture in mobile telemedicine. In: Martinez L, Gomez C, editors. Telemedicine in the 21st Century. Nova Science Publishers; USA, 2008. pp. 187-201

[21] Lin CF, Wang SE, Lu YC, et al. Mobile cloud-based blood pressure healthcare for education. In: Bonney W, editor. Mobile Health Technologies-Theories and Applications. Intech Science Publishers; Croatia, 2016. pp. 99-114